Appl. Sci. Converg. Technol. 26(5): 129-132 (2017)
http://dx.doi.org/10.5757/ASCT.2017.26.5.129

Research Paper

Controllable Growth of Single Layer MoS_2 and Resistance Switching Effect in Polymer/MoS_2 Structure

Sung Jae Park, Dongil Chu, and Eun Kyu Kim*
Department of Physics and Research Institute for Natural Sciences, Hanyang University, Seoul 04763, Korea

Received July 12, 2017; revised September 21, 2017; accepted September 26, 2017

Abstract We report a chemical vapor deposition approach and optimized growth condition to the synthesis of single layer molybdenum disulfide (MoS_2). Obtaining large grain size with continuous MoS_2 atomically thin films is highly responsible to the growth distance between molybdenum trioxide source and receiving silicon substrate. Experimental results indicate that triangular shape MoS_2 grain size could be enlarged up to > 80 um with the precisely controlled the source-to-substrate distance under 7.5 mm. Furthermore, we demonstrate fabrication of a memory device by employing poly(methyl methacrylate) (PMMA) as insulating layer. The fabricated devices have a PMMA-MoS_2/metal configuration and exhibit a bistable resistance switching behavior with high/low-current ratio around 10^3.

Keywords: MoS_2, CVD, Controllable grain size, Memory

I. Introduction

After discovery of grapheme, transition metal dichalcogenides(TMDs) have received much attention due to their interesting electronic and optical properties for application to novel devices [1-3]. One of the most investigated material, molybdenum disulfide (MoS_2) present a direct band gap (~1.8 eV) in the monolayer form and revealed an indirect band gap (~1.2 eV) in the bulk state which makes them promising for future logic device beyond the grapheme. The systems for synthesizing MoS_2 have been widely examined in the past few years. Chemical vapor deposition (CVD) approach has been proved as a confident system in synthesizing large area and high quality single layer TMD layer [8-15]. The common technique for growing MoS2 layer was deposition of molybdenum trioxide (MoO_3) or Mo on a silicon dioxide (SiO_2) substrate and followed by sulfurization by a sulfur vapor at high temperature. The MoS_2 grown by sulfurization method usually has high surface coverage and good uniformity. However, the small grain size of the epi-layer is the major disadvantage. For the certain device application, large grain size and high surface coverage of the synthetic layer is the most important.

In this work, we have successfully synthesized MoS_2 thin films with the thickness from single layer to few layers by using CVD system. In order to increasing grain size of single layer MoS_2 the growth distance between substrate and sources (such as MoO_3) was optimized. Furthermore, the CVD grown MoS_2 thin film is integrated into resistance switching memory, while MoS_2 layer in this device takes on a role as a charge trapping and detrapping layer with dielectric materials encapsulation.

II. Experiments

CVD synthesis of MoS_2 was performed by using 99.999% purity MoO_3 powder and 99.999% purity sulfur (S) powder as the reactant materials. The concentration of the S vapor must be much higher than the MoO_3 precursor to complete the sulfurization. To accomplish this, 10 mg MoO_3 powder was put in the alumina boat, and the SiO_2 (270 nm-thick)/Si substrate (~1.5 × 1.5 cm^2) was placed on the alumina boat. The alumina boat was placed at the center of the heating zone of a 2-inch quartz tube. A total of 100 mg S of powder was supplied in another alumina boat and was located upstream relative to the carrier gas flow direction from the MoO_3 source. The heating zone was heated up to a temperature of 690°C at a heating rate of 16°C/min under argon atmosphere under a 100-sccm flow rate. Argon gas played as the carrier gas to make the diffusion of S vapor to the heating zone. The gas flow rate was set to be constant at 10-sccm after 690°C. When the growing procedure starts, the heating zone temperature was retained at 690°C for 5 minutes. The MoO_3 sources formed MoO_{3-x} and further reacted to the S vapor to synthesis MoS_2 film at 690°C. The single layer MoS_2 thin film was grown by diffusing these sub-oxide compounds to the substrate. For the fabrication of the memory devices,

*Corresponding author
E-mail: ek-kim@hanyang.ac.kr

synthesized MoS_2 film was coated with poly(methyl methacrylate) (PMMA) solution using spin coater. The PMMA films acted as both of the supporting layer for the transfer process and dielectric materials in the device. The PMMA-MoS_2 stack was further transferred onto a silicon substrate in which a gold film coated. A top aluminum electrodes (100 nm) were deposited by using thermal evaporator on PMMA-MoS_2 layer to form Al-PMMA-MoS_2-Au configuration.

To characterize the structure of MoS_2 film, Raman measurement was conducted with laser excitation energy of 532 nm. X-ray photoelectron spectroscopy (XPS) was used for examining the chemical composition, crystal structure, and residual elements. An optic microscopy was employed to determine the grain size and thickness. Current-voltage (I-V) characteristic measurements were carried out by using a semiconductor parameter analyzer.

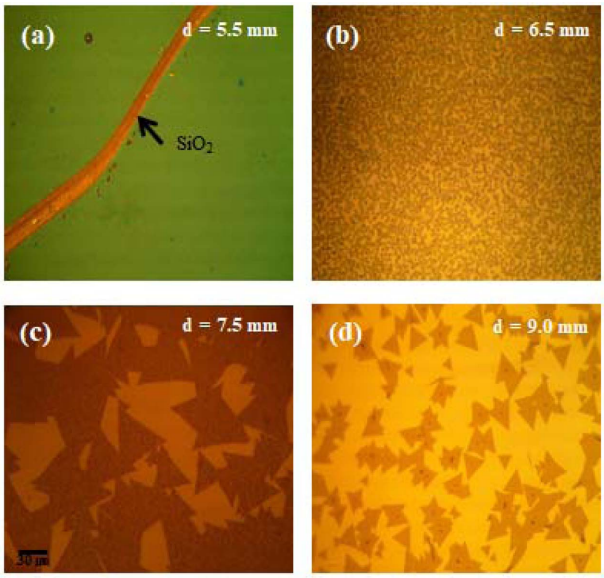

Figure 1. Optical images of the MoS2 product (a-d) at the difference growth substrate.

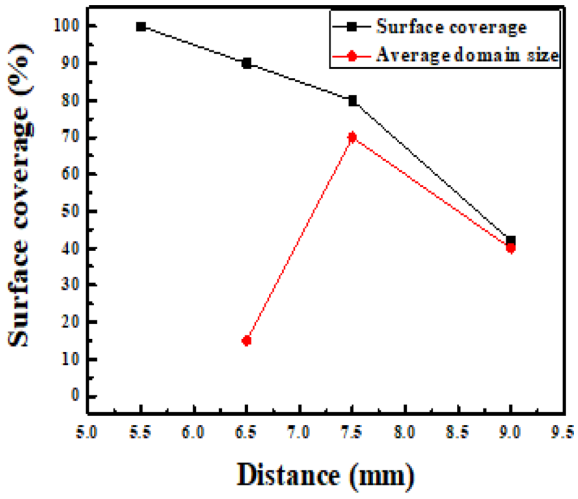

Figure 2. Surface coverage and average domain size at difference distance from source to substrate.

III. Result and Discussion

Controlling the layer number and grain size of the CVD-grown MoS_2 layer is achieved by adjusting the distance from MoO_3 sources to substrate. Figure 1(a-d) shows the optical image of the CVD-grown MoS_2 at various distances from 5.5 to 9.0 mm. Figure 1(a) shows the typical few layer MoS_2 film grown, the substrate is fully covered by MoS_2 thin film. For the short distance (~5.5 mm), the high concentration of the MoO_3 gaseous deposited on the substrate directly. The higher gaseous MoS_2 assured that the much chemical reaction occurred with the relatively short distance. When increasing the distance to be 6.5 mm, The triangular shape MoS_2 fully cover the growth substrate as shown in Fig. 1(b). In this distance, the space is not allowed for growing the large grain. The average grain size is around 10 μm as increase the distance between sources to substrate. Figure 1(c) shows the resulting MoS_2 layer when the distance set to be 7.5 mm. The overall surface coverage has been reduced from 90 to 85%, but the average grain size has increased from 10 um to 80 um. The triangular shapes are presented at the edge of substrate where nuclei density is relatively low. It also means enough space is essential for growing the large grain size of MoS_2. Some overlying triangular shape flakes embody the original process of the formation of the MoS_2 thin film. It is decent displaying that the large grain size MoS_2 flake (> 80 μm) has been well synthesized at this distance. As the distance increases more than 7.5 mm, the overall surface coverage is decreased to 45% and the average domain size also decreased to 40 μm (Fig. 1(d)). The low concentration of gaseous MoS_2 failed to supply enough sources gas, causing the lower surface coverage and small grain size. Figure 2 shows the average domain size and the surface coverage as a function of distance from source to growth substrate. The surface coverage accommodates 100% at the 5.5 mm distance and slightly decreases as increasing the distance. This is because that the high gaseous MoS_2 provides both high-density nuclei and plentiful source gas supply. Plentiful gaseous MoS_2 insures that the high-density nuclei can keep synthesizing until the grain merge each other. On the other hand, the moderate low-density nuclei and gaseous help to synthesize large grain size

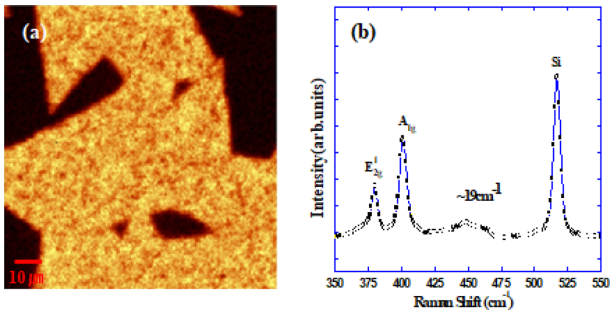

Figure 3. (a) Raman mapping image of MoS_2 grown by CVD method, (b) Raman spectra of MoS2 grown by CVD method.

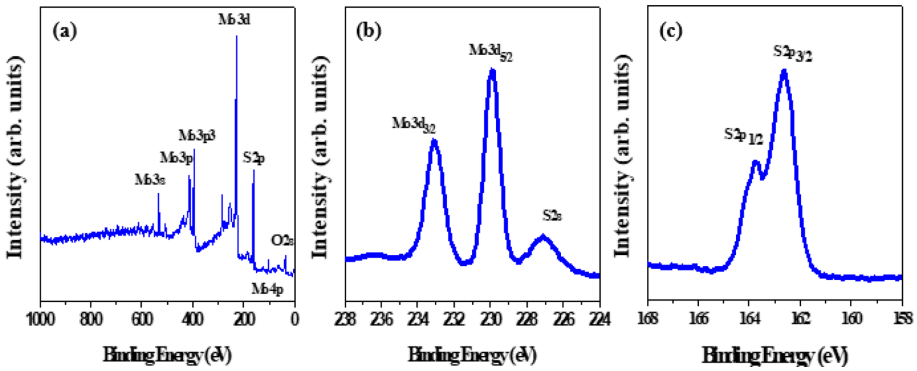

Figure 4. (a) XPS survey scans for CVD-MoS_2 and (b) the XPS spectra of the Mo 3d state, (c) S 2s state.

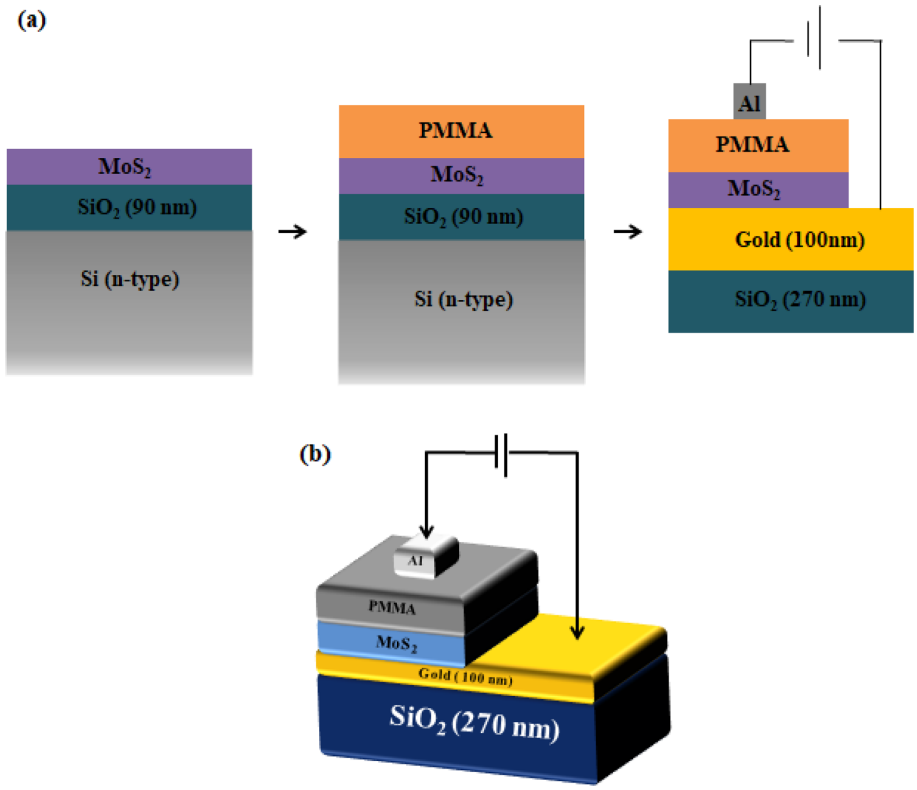

Figure 5. (a) Transfer process of the CVD-MoS_2 for the fabrication of memory device. (b) Schematic diagram of the PMMA/MoS_2/gold structure as a memory device.

without decreasing the surface coverage. However, in relatively long distance (more than 7.5 mm), the average domain size and surface coverage both reduced.

Figure 3(a) and (b) show the Raman mapping image of MoS_2 and Raman spectra of the CVD-grown MoS_2, respectively. It shows that MoS_2 with around 80 um of grain size was synthesized on the substrate. Raman spectra demonstrated two characteristic peaks at 402.27 and 383.18 cm^{-1}, which are A_{1g} and E^1_{2g} modes, respectively. The E^1_{2g} mode is correlated with the vibration of the Mo-S bond along the basal plane. While the A_{1g} mode is due to the vibration of the sulfur atoms along the vertical axis. The difference between the E^1_{2g} and A_{1g} peak was used to confirm the thickness of the MoS_2 layer, and it was found to be 19.09 cm^{-1}, corresponding to a single layer structure [16]. The full width at half maximum (FWHM) of the E^1_{2g} peak is known as an indicator for crystalline quality [17]. The FWHM of E^1_{2g} peak from the synthesized MoS_2 is 4.35 cm^{-1} which was correlated to the high quality crystalline of MoS_2.

The surface chemistry of the CVD-grown MoS_2 was characterized by XPS measurements as shown in Fig. 4. From the survey scans of Fig 4(a), the Mo, S and O peaks can be found. In Fig. 4(b), the XPS spectra shows two peaks at 229.7 and 233.6 eV, corresponding to the Mo $3d_{3/2}$ and Mo $3d_{5/2}$ state, respectively. Fig. 4(c) shows the binding energies of S $2p_{1/2}$ and S $2p_{3/2}$ at 163.16 and 162.53 eV, respectively. The 2H-MoS_2 crystal for Mo 3d shows two peaks at 229.7 and 233.6 eV that can be attributed to the doublet Mo $3d_{5/2}$ and $3d_{3/2}$ [18]. The data of 229.3 and 233.2 eV from the CVD-grown MoS_2 are in agreement with the reported data [19]. Therefore, it is clear that our

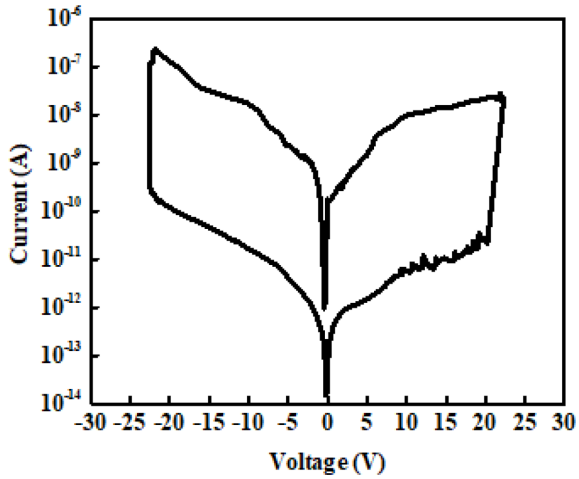

Figure 6. I-V characteristic of fabricated memory device.

CVD grown MoS_2 samples have a single layer with 2H-MoS_2 crystalline structure. We also found that the elemental concentrations of Mo and S are 30.25% and 69.15%, with a ratio of 1.00:2.28. These data further prove the chemical composition of MoS_2.

Figure 5(a) show the transfer process of the MoS_2 thin films for the fabrication of memory device. PMMA solution was coated by using spin coater. And then, PMMA/MoS_2/SiO_2/Si sample was immersed in buffered oxide etch (BOE) solution for etching the SiO_2 layers. After removing the SiO_2 layers, PMMA/MoS_2 structure floating on the BOE solution was deposited on the gold/SiO_2/Si substrate. Figure 5(b) displays a schematic diagram of the memory device with Al/PMMA/MoS_2/Gold structure. In this memory device, gold acts as the electrode and PMMA/MoS_2 structure is used for charges trapping materials.

Figure 6 shows a typcial I-V characteristic of the device. The current gradually increased with increasing the applied voltage from 0 to 22 V and then abrupt increase in current from 0.0308 nA to 31.047 nA with a high resistance state/low resistance state ratio up to 10^3. This memory characteristic of the device is contributed to charge trapping and detrapping between MoS_2 and PMMA. There are highest occupied molecular orbital (HOMO) and lowest unoccupied molecular orbital (LUMO) levels of PMMA with 7.3 eV and 1.8 eV, respectively [20]. MoS_2 has 3.0-4.30 eV electron affinities with a 1.3-1.8 eV band gap. Consequently, PMMA/MoS_2 structures will build a carrier injection barrier as applying voltage. To develop this memory device, a selection of dielectric materials is still required to be optimized which will amplify the I-V characteristic. This PMMA/MoS_2/gold structure device show efficient memory characteristic. Hence, PMMA/MoS_2/Metal structure can be used in the next generation non-volatile memory device. However, the further studies on the endurance and retention data should be needed to confirm the usefulness of the 2D material for the resistive switching memory device.

IV. Conclusions

In summary, we have demonstrated the optimized growing method for MoS_2 single layer. The thin films coverage is highly dependent on the distance between source and substrate. We have successfully grown high surface coverage and large grain size exceeding 80 um by carefully adjusting the distance. We also fabricated the Al/PMMA/MoS_2/Metal structure as a resistive sensitive memory device. Typical electrical switching memory effect was observed in this device with a 10^3 current change. The PMMA/MoS_2 structure system can be significant platform for future generation data storage device.

References

[1] K. S. Novoselov, A. K. Geim, S. V. Morozov, D. Jiang, Y. Zhang, S. V. Dubonos, I. V. Grigorieva, and A. A. Firsov, Science. 306 (2004) 666.
[2] K. I. Bolotin, K. J. Sikes, Z. Jiang, M. Klima, G. Fudenberg, J. Hone, P. Kim, and H. L. Stormer, Solid State Communication, Solid State Commun. 146 (2008) 351.
[3] M. Liu, X. Yin, E. Ulin-Avila, B. Geng, T. Zentgraf, L. Ju, F. Wang, and X. Zhang, Nature. 474 (2011) 64.
[4] Q. H. Wang, K. Kalantar-Zadeh, A. Ais, J. N. Coleman & Strano, Nat. Nanotechnol. 699-712 (2012) 7.
[5] M Chhowalla, et al. Nat Chem. 263 (2013) 5.
[6] M. Xu, T. Liang, M. Shi & H. Chen, Chem. Rev. 2766 (2013) 113.
[7] R. Ganatra & Zhang, and Q. ACS nano. 4074 (2104) 8.
[8] B. Radisavljevic, A. Radenovic, J. Brivio, V. Giacometti, and A. Kis, Nat. Nanotechnol. 6 (2011) 147.
[9] Y. J. Zhan, Z. Liu, S. Najmaei, P. M. Ajayan, and J. Lou, Small. 8 (2012) 966.
[10] Y. F. Yu, C. Li, Y. Liu, L.Q. Su, Y. Zhang, and L.Y. Cao, Sci. Rep. 3 (2013) 1866.
[11] Y. C. Lin, W. J. Zhang, J. K. Huang, K. K. Liu, Y. H. Lee, C. T. Liang, C. W. Chu, and L. J. Li, Nanoscale. 4 (2012) 6637.
[12] Y. H. Lee, X. Q. Zhang, W. J. Zhang, M. T. Chang, C. T. Lin, K. D. Chang, Y. C. Yu, J. T. W. Wang, C. S. Chang, L. J. Li, and T. W. Lin, Adv. Mater. 24 (2012) 2320.
[13] A. M. van der Zande, P. Y. Huang, D. A. Chenet, T. C. Berkelbach, Y. M. You, G. H. Lee, T. F. Heinz, D. R. Reichman, D. A. Muller, and J. C. Hone, Nat Mater. 12 (2013) 554.
[14] R. Gatensby, N. McEvoy, K. Lee, T. Hallam, N.C. Berner, E. Rezvani, S. Winters, M. O'Brien, and G.S. Duesberg, Appl. Surf. Sci. 297 (2014) 139.
[15] J. Z. Ou, A. F. Chrimes, Y. C. Wang, S. Y. Tang, M. S. Strano, and K. Kalantar-zadeh, Nano Lett. 14 (2014) 857.
[16] H. Li, Q. Zhang, C. C. R. Yap. B. K. Tay, T. H. T. Edwin, A. Olivier, and D. Baillageat, Adv. Funct. Mater. 22 (2012) 1385.
[17] Y. Yu, C. Li, Y. Liu, L. Su, Y. Zhang, and L. Cao, Sci. Rep. 3 (2013) 1866.
[18] Y. Lee, J. Lee, H. Bark, I. K. Oh, G. H. Ryu, Z. Lee, H. Kim, J. H. Cho, J. H. Ahn, and C. Lee, Nanoscale. 6 (2014) 2821.
[19] Y. M. Shi, J. K. Huang, L. M. Jin, Y. T. Hsu, S. F. Yu, L. J. Li, and H. Y. Yang, Sci. Rep. 3 (2013) 1839.
[20] Y. J. Yun, C. pearson, and M. C. Petty, J. Appl. Phys. 105 (2009) 034508.